OBTAINING THE CONSTITUTIVE TENSILE RELATION OF CONCRETE THROUGH INVERSE ANALYSIS

José Luiz Antunes de Oliveira e Sousa[1] and Ravindra Gettu[2]
[1]Universidade Estadual de Campinas, 13083-852 Campinas, SP, Brazil
[2]Universitat Politècnica de Catalunya, Barcelona 08034, Spain

ABSTRACT

This paper deals with the determination of a stress-crack opening (σ-w) curve for the characterization of the fracture behavior of plain and fiber reinforced concretes. The objective is to provide a constitutive model for the application of cohesive crack models in the analysis of structural members. Several researchers have proposed the use of beam tests to obtain the σ-w relation indirectly using inverse analysis. In the strategy described here, an error function is defined as the integral of the squared differences between a numerically- or analytically-obtained load-crack opening (P-CMOD) curve and the corresponding curve resulting from three-point bend tests of notched prismatic specimens. Optimization techniques are employed to find the set of σ-w parameters that leads to the minimum error. The strategy has been implemented in an object-oriented code, which is capable of handling any σ-w curve description. The current implementation uses a third party analytical code for computing the P-CMOD curve corresponding to a trial σ-w set of parameters. Implementation of new σ-w models or different schemes for computation of P-CMOD curves, e.g., using the finite element method, is straightforward. Example applications are presented.

1 INTRODUCTION

Simulation of the nonlinear fracture behavior of concrete using a cohesive crack model, such as that proposed by Hillerborg et al. [1], requires a stress-crack opening relation (σ-w) to represent the fracture processes that occur ahead of the traction-free crack. In this process zone, cohesive stresses occur due to bridging, microcracking and aggregate interlock. One experimental approach for the determination of the σ-w curve is the uniaxial tension test, performed under displacement control. Due to difficulties with the experimental setup for such tests, many researchers [2-5] have proposed the use of other simpler test setups, such as the bending test performed on notched prismatic specimens. These alternative setups, however, do not yield the σ-w curve directly, requiring inverse analysis to obtain it from the load-crack mouth opening (P-CMOD) or load-displacement data from the laboratory test. In the inverse analysis procedure, a set of parameters is provided as a seed for an iterative process, and a numerical or analytical model is used to determine a corresponding P-CMOD curve, which is compared with the P-CMOD curve obtained from the laboratory test. Optimization techniques are used to determine the next trial, based on a predefined error measure, which is the objective function in the process. In this paper, the computational aspects of the inverse analysis approach and its implementation are discussed through examples.

2 DETERMINING THE P-CMOD CURVE FOR A GIVEN σ-w CURVE

The fitting of a set of parameters that reproduces the P-CMOD obtained in the laboratory is performed by an error minimization procedure, as follows: starting with a seed set of parameters supplied by the user, determining a new trial set based on the error function behavior in the neighborhood of this set of parameter, and stopping when the minimum is reached.

For each trial set, and for auxiliary sets used to evaluate error function behavior in their neighborhoods (derivatives), P-CMOD curves have to be generated and compared to the target in order to produce the corresponding value of the error function ζ_{sqr}. Many strategies are possible for this task. Finite element models, available in academic or commercial packages, generate reliable solutions, although they are time consuming. Since these computations are performed many times for the fitting procedure, analytical or quasi-analytical models seem to be more adequate, despite the expected loss of accuracy. In the example applications presented in this paper, a quasi-analytical formulation based on the cracked hinge model, developed by Stang et al. [6,7], was used. This formulation was seen to be very efficient, yielding results that were close to those obtained from finite element packages, without needing the same computation time.

3 BEHAVIOR OF THE ERROR MEASURE

Given a trial set of parameters, represented by the vector **p**, the error at a point of the P-CMOD curve, corresponding to a given crack mouth opening (CMOD), represented by the scalar v, is defined as:

$$\delta(\mathbf{p},v)=P_{trial}(\mathbf{p},v)-P_{\exp}(v) \tag{1}$$

$P_{trial}(\mathbf{p},v)$ load corresponding to the given CMOD obtained from the numerical or analytical model applied to a trial set of parameters;

$P_{\exp}(\mathbf{p},v)$ load corresponding to CMOD obtained from experimental P-CMOD data;

v crack mouth opening displacement (CMOD)

The error measure, suitable for the use of optimization algorithms, is given by

$$\zeta_{sqr}(\mathbf{p})=\int_0^{v_{\max}}\delta(\mathbf{p},v)^2\psi(v)\,dv \tag{2}$$

$\Psi(v)$ weighting function to give unequal importance to portions of the P-CMOD curve

v_{max} upper limit in the v interval, selected by the user

For the use of optimization algorithms it would be convenient if the convexity of this function could be proven. This would lead to the existence and uniqueness of a global minimum, and its determination would be relatively straightforward with the algorithms available in the literature or in computational packages. However, a close look at the behavior of a typical problem with $\mathbf{p}\in R^2$ leads to the conclusion that convexity cannot be proven. The surface plot shown in Figure 1, corresponding to a test on a notched beam specimen subject to a three-point loading, makes it clear that inflexion may occur far away from the minimum. Furthermore, in the close neighborhood of the minimum, convergence may become difficult because of the non-smoothness of the experimental P-CMOD curve. However, if an adequate search direction algorithm and appropriate tolerances are adopted, a reliable minimum can be found in most cases.

4. HANDLING CURVES IN FIT3PB

P-CMOD curves are handled as a set o n (CMOD, P) pairs. In order to allow simple computation of error, the experimental P-CMOD curve is recomputed in such a way that its description uses a given number (n) of pairs, which will be the same in the computation of the corresponding numerical curve. This strategy enables easy numerical evaluation of the integrals involved in ζ_{sqr}.

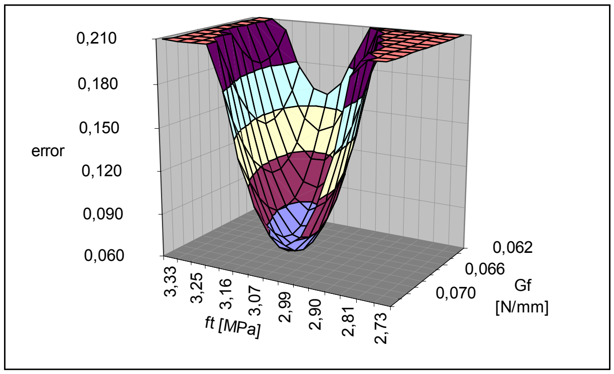

Figure 1 Three-dimensional plot of the fitting error ζ_{sqr} as a function of f_t and G_f

5. DETERMINING THE MINIMUM FROM A TRIAL SET OF σ-w PARAMETERS

The strategy to determine the minimum of the error function ζ_{sqr} is based on the following tasks:

a. Starting from a seed trial set of softening parameters, the error ζ_{sqr} is computed;
b. If the error ζ_{sqr} is within the tolerance, the trial set is the minimum sought, else the next steps should be followed;
c. First and second partial derivatives of ζ_{sqr} are numerically evaluated, resulting in an estimation of the function gradient and the Hessian matrix;
d. If the Hessian matrix is positive definite, the search direction is that indicated by a Newton-Raphson scheme, otherwise it is the opposite to that indicated by the gradient;
e. Once the search direction is determined, a line search algorithm is used to find the minimum in that direction;
f. Repeat steps (a) to (f) until the error is within the predefined tolerance or a maximum number of steps is reached;
g. Evaluate the quality of the solution by computing the error using the alternative definition of the error given by

$$\zeta_{abs}(\mathbf{p}) = \int_0^{v_{\max}} \left|\delta(\mathbf{p},v)\right| dv \Big/ \int_0^{v_{\max}} P_{\exp}(v)\, dv \tag{3}$$

which is non-dimensional and, for the three point bending test, roughly yields the fraction of the fracture energy that corresponds to the error in the comparison between the P-CMOD curves obtained by the analytical or numerical model and the one obtained from the laboratory tests.

6. DETERMINATION OF THE GRADIENT AND THE HESSIAN MATRIX

The strategy to determine partial derivatives of the error function ζ_{sqr} in the current implementation is based on a finite difference scheme. Considering a pair of parameters (p_i, p_j), and five other pairs, as indicated in Figure 2, where Δp_i and Δp_j are parameters variations defined by the user, a quadratic polynomial $\zeta\left(p_i, p_j\right)$ is obtained by interpolation to six points defined in the plane $p_i \times p_j$ in Figure 2. The components of the gradient and the Hessian matrix are evaluated by:

$$g_i = \frac{\partial \zeta\left(p_i, p_j\right)}{\partial p_i} \text{ and } H_{ij} = \frac{\partial^2 \zeta\left(p_i, p_j\right)}{\partial p_i\, \partial p_j} \tag{4}$$

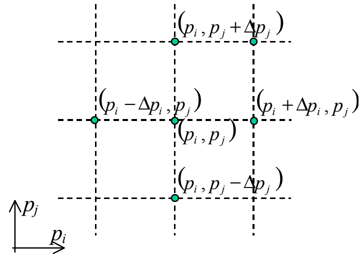

Figure 2 Scheme for partial differentiation

7. PROCEDURE FOR THE MINIMIZATION OF THE FUNCTION ζ_{sqr}

An iterative procedure is followed for the minimization of the ζ_{sqr} function, starting with a seed trial set of parameters, $\mathbf{p}^{(0)}$, supplied by the user. In a typical iterative step *k*, the direction of decrease $\mathbf{d}^{(k)}$ is determined (i.e., search direction) from the partial derivatives of the objective function at the point $\mathbf{p}^{(k)}$. Line search algorithms are then applied to determine the minimum of the objective function along the line defined by $\mathbf{p}^{(k)}$ and $\mathbf{d}^{(k)}$. The parameters corresponding to this minimum are the trial set $\mathbf{p}^{(k+1)}$ for the next iteration. The iterative process stops when the difference between $\zeta_{sqr}(\mathbf{p}^{(k+1)})$ and $\zeta_{sqr}(\mathbf{p}^{(k+1)})$ is within a given tolerance, or a given limiting number of iterations is reached. The alternative error measure $\zeta_{abs}(\mathbf{p}^{(k+1)})$ is returned to the user. The sections to follow describe search direction and line search algorithms (see Luenberger, [8]).

7.1. Determination of the search direction

In an iteration (k), provided the gradient $\mathbf{g}^{(k)}$ of the objective function ζ_{sqr} at the current trial point $\mathbf{p}^{(k)}$ is not null, a direction of decrease is given as that opposite to the gradient $\mathbf{d}^{(k)} = -\mathbf{g}^{(k)}$. A line search algorithm applied along the line defined by $\mathbf{p}^{(k)}$ and $\mathbf{d}^{(k)}$ results in new trial point $\mathbf{p}^{(k+1)}$. The convergence rate improves significantly if the search direction takes into account the second partial derivatives, according to a Newton-Raphson scheme: $\mathbf{d}^{(k)} = -\left(\mathbf{H}^{(k)}\right)^{-1}\mathbf{g}^{(k)}$. This strategy, however, is valid only when the Hessian matrix is positive definite. As this condition is not satisfied everywhere in the $\mathbf{p}$ domain, the positive definiteness of the Hessian matrix is tested to decide which expression for $\mathbf{d}^{(k)}$ should be used.

7.2. Minimization along the search direction

Many algorithms for minimization along a line (i.e., line search) are available in the literature (e. g. [8]). In general, they are based on function evaluation for three or more points, attempting to identify the minimum in an interval within a given tolerance. The strategy in the current implementation combines the Golden Section algorithm with a Parabolic Fitting algorithm.

8. EXAMPLE APPLICATIONS

In the first example application, three softening models (i.e., shapes of the σ-w curve), described in Figure 3, have been chosen for the plain concrete. The results obtained are given in Figure 4. The P-CMOD curves clearly show that the linear softening model leads to a poor fit, while both the Hordijk and bilinear models lead to lower errors, with the latter, with four parameters, yielding the least error. However, the Hordijk model [9] presented a sufficiently close solution with only two parameters: the tensile resistance f_t and the fracture energy G_f.

Softening models suitable for fiber reinforced concrete, with two, three, four and six parameters, are plotted in Figure 5. Results from the inverse analysis for these models are given in Figure 6. The application of the drop-constant model resulted in a poor fit at the peak load. Conformity with the P-CMOD curve is significantly improved when a slope is introduced in the model after the peak, even if the tail is constant (e.g. in the sloped-constant model). Further enhancement is achieved with the bilinear and trilinear models.

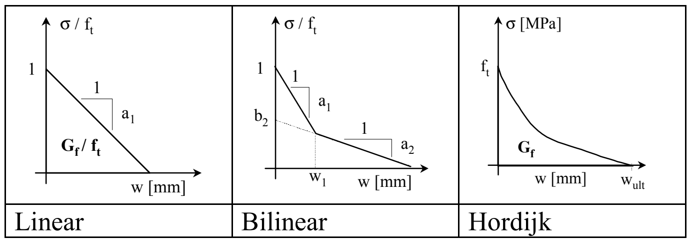

Figure 3 Softening models for plain concrete

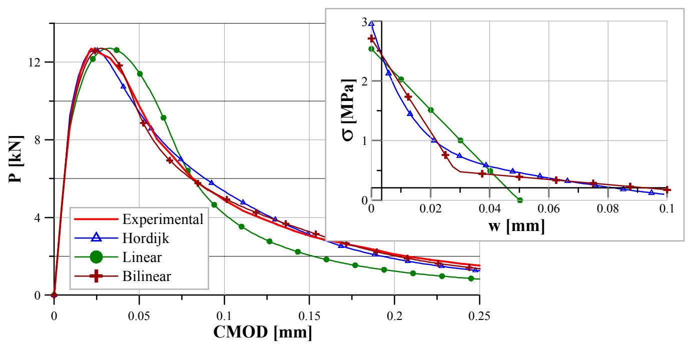

Figure 4 Comparison of softening models and fits for plain concrete

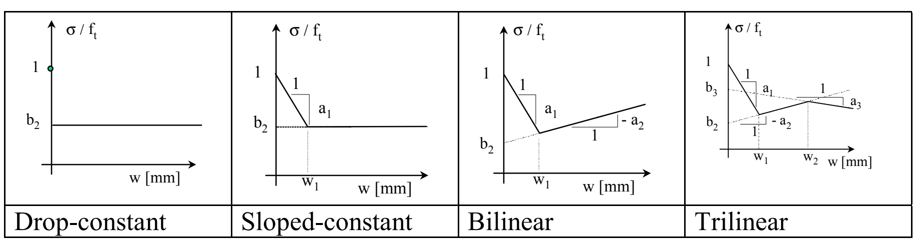

Figure 5 Softening models for fiber reinforced concrete

9. CONCLUSIONS

An optimization strategy for the determination of the σ-w curve for plain and fiber reinforced concretes has been presented. The strategy has been implemented in a software program and applied to both plain and fiber reinforced concretes. The resulting σ-w curves, when used as input data for computing the P-CMOD curve for notched prismatic beam specimens, lead to a minimum error when compared to the corresponding experimental curve. A discussion of data manipulation and quality of the results has been presented, suggesting the adequacy of the proposed strategy.

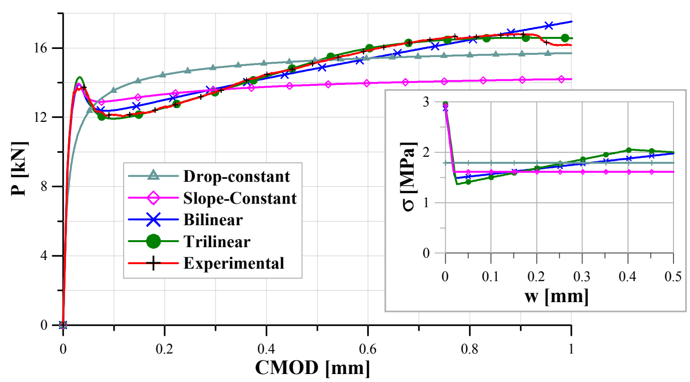

Figure 6 Comparison of softening models for fiber reinforced concrete

10. REFERENCES

1 HILLERBORG, A., MODEER, M., PETERSSON, P-E. (1976) Analysis of crack formation and crack growth in concrete by means of fracture mechanics and finite elements, **Cem. Concr. Res.**, V. 6, pp.773-782.
2 GUINEA, G., PLANAS, J., ELICES, M. (1994) A general bilinear fit for the softening curve of concrete, **Mater. Struct**., V. 27, pp. 99-105.
3 KITSUTAKA, Y., OH-OKA, T. (1998) Fracture parameters of high-strength fiber reinforced concrete based on poly-linear tension softening analysis, **Fracture Mechanics of Concrete Structures,** Eds. H.Mihashi & K.Rokugo, Aedificatio Publ., Freiburg, Germany, pp. 455-464.
4 KOOIMAN, A.G., VAN DER VEEN, C., WALRAVEN, J.C. (2000) Modelling the postcracking behaviour of steel fibre reinforced concrete for structural design purposes, **Heron**, V. 45, No. 4, pp. 275-307.
5 ROELFSTRA, P.E., AND WITTMANN, F.H. (1986) Numerical method to link strain softening with failure of concrete, **Fracture Toughness and Fracture Energy of Concrete,** Ed. F.H.Wittmann, Elsevier Science, pp. 163-175.
6 STANG, H., OLESEN, J.F. (1998) On the interpretation of bending tests on FRC materials, **Fracture Mechanics of Concrete Structures**, Eds. H. Mihashi and K. Rokugo, Aedificatio Publ., Freiburg, Germany, pp. 511-520.
7 STANG, H., OLESEN, J.F. (2000) A fracture mechanics based design approach to FRC, **Proc. Fifth RILEM Symposium on Fibre-Reinforced Concretes**, Eds. P. Rossi and G.Chanvillard, RILEM, Cachan, France, pp. 315-324.
8 LUENBERGER, D.G. (1984) **Linear and Nonlinear Programing**, Addison-Wesley Publishing Company, 491 p.
9 HORDIJK, D.A. (1991) **Local approach to fatigue of concrete,** Doctoral thesis, Delft University of Technology, The Netherlands.

ACKNOWLEDGMENTS

The support provided by the Brazilian institutions FAPESP - Fundação de Amparo à Pesquisa do Estado de São Paulo (grant 00/10616-9) and CNPq - Conselho Nacional de Desenvolvi-mento Científico e Tecnológico (grant 30.1401/92-6), and the Spanish MCYT projects PB98-0298 and MAT2003-5530 is gratefully appreciated. The collaboration was made possible by the Spanish-Brazilian Program for Inter-University Cooperation, funded by MEC grant PHB2002-0053 (in Spain), and CAPES grant CGCI-49/03 (in Brazil)